



**Advances in Research**

Volume 26, Issue 1, Page 101-109, 2025; Article no.AIR.129614  
ISSN: 2348-0394, NLM ID: 101666096

# Finite Element Analysis of Temperature Effects on Underground Large-Diameter Concrete Cylinders Using ABAQUS

Fuzheng Chen <sup>a\*</sup>

<sup>a</sup> North China University of Water Resources and Electric Power, Zhengzhou-450045, Henan, China.

## Author's contribution

The sole author designed, analyzed, interpreted and prepared the manuscript.

## Article Information

DOI: <https://doi.org/10.9734/air/2025/v26i11237>

## Open Peer Review History:

This journal follows the Advanced Open Peer Review policy. Identity of the Reviewers, Editor(s) and additional Reviewers, peer review comments, different versions of the manuscript, comments of the editors, etc are available here: <https://www.sdiarticle5.com/review-history/129614>

Original Research Article

Received: 06/11/2024

Accepted: 08/01/2025

Published: 14/01/2025

## ABSTRACT

With the increasing demand for storage capacity, the diameter of silos has also been continuously increased. For this kind of large-diameter concrete cylinder, the temperature load has a great influence, especially the cylinder structure located underground, and the stress characteristics are more complicated under the influence of earth pressure and gradient temperature. This study investigates the stress distribution and deformation in underground large-diameter concrete cylinders under temperature loads using finite element analysis with ABAQUS. By simulating temperature changes through boundary conditions, the research identifies critical stress patterns, particularly the significant hoop tensile stress observed during temperature decreases, which peaks at 2.75 MPa. These findings emphasize the need for enhanced tensile capacity in specific regions of the structure. The results provide valuable insights for optimizing the design and ensuring the structural integrity of underground concrete cylinders under varying thermal conditions.

\*Corresponding author: E-mail: [chenfuzheng666@163.com](mailto:chenfuzheng666@163.com);

**Cite as:** Chen, Fuzheng. 2025. "Finite Element Analysis of Temperature Effects on Underground Large-Diameter Concrete Cylinders Using ABAQUS". *Advances in Research* 26 (1):101-9. <https://doi.org/10.9734/air/2025/v26i11237>.

**Keywords:** *Underground large-diameter concrete cylinder; temperature effects; finite element method; ABAQUS.*

## 1. INTRODUCTION

The impact of temperature variations on the structure of large-diameter concrete cylinders is significant. Kong et al., (1998) studied the temperature stresses caused by solar radiation temperature differences, seasonal temperature differences, and internal and external temperature differences in large-diameter reinforced concrete silos, and provided the magnitude and calculation methods that should be considered in design. Xia et al., (2006) conducted a finite element analysis on giant reinforced concrete coal storage silos under ambient temperature conditions and found that the impact on the hoop stress of the silo when the external environment cools down is greater than when it heats up. Using the finite element analysis software ANSYS, Morán J M et al. (2006, 2005) conducted a computational analysis of the stress distribution in silo structures subjected to temperature differences. The results of this analysis indicate that when the temperature difference between the interior and exterior of the silo exceeds 20°C, the structural internal forces within the silo significantly increase. Zhang (2010) utilized the ANSYS finite element analysis software to apply temperature loads to both full and empty steel silos, and conducted computational analyses on them. Under temperature loads, due to the significant constraints imposed on the structure, the resulting temperature stresses are considerable. Therefore, in the structural design of both full and empty silos, the effect of temperature cannot be neglected and must be fully considered. Guo (2018), through field tests conducted on coal storage silos in severely cold regions, studied and analyzed the evolution of stress in silos under conditions of temperature rise and fall. Comprehensive comparisons were made of the stress patterns of the structure under different temperature effects, and the temperature-stress response relationship of the silo was summarized. By analyzing the hydration heat generated during the construction period of mass concrete and comparing it with actual measurement data, the design of silo structures was optimized. Zhao et al. (2018) conducted field measurements of the temperature distribution in concrete silos under solar radiation. They established a finite element model and analyzed the influence of meteorological parameters, silo size, and reference temperature on the temperature effects

of the silo. The results showed that the temperature gradient exhibits obvious nonlinearity along the wall thickness direction. For silos with a thickness greater than 30 cm, the steady-state method overestimates the temperature effect, and it is recommended to consider the temperature effect of large silos using a nonlinear temperature gradient. Khalifa et al., (2019) evaluated the impact of thermal loads on the design of silo walls in terms of applied forces and stresses, finding that nonlinear analysis is more accurate than linear analysis. The research results on hoop stresses exhibited different patterns with temperature differences, silo radii, and insignificant silo wall thicknesses. Peng and Fan (2020), relying on a circular prestressed reinforced concrete coal storage silo of a 2×660 MW coal-fired power plant in Inner Mongolia, simulated the mechanical characteristics of the silo structure under storage load, temperature effects, and prestress loads, providing assistance for design work. Bai et al. (2022) studied the strength, peak strain, and failure characteristics of concrete under four temperature gradients. The damage mechanism of concrete was further revealed through acoustic emission ring-down counts and b-values. The results showed that as the temperature increases, the concrete strength rapidly decreases and the peak strain increases. As the temperature gradient increases, the failure characteristics of concrete gradually shift from brittleness to ductility. Wang et al. (2022) introduced the research results on the cracking behavior of early-age mass concrete in large-diameter pipelines during the construction period and monitored the temperature and strain of the concrete. The study found that a diameter-to-margin ratio or diameter-to-spacing ratio not exceeding 1/3 is sufficient to prevent additional cracking risks in concrete due to the presence of the pipeline. Zhangabay et al. (2023) presented experimental research results on the working characteristics of prestressed shells considering the impact of temperature loads on the initial structural state. As the temperature load on the structure increases, the tension level of the prestressed structure decreases. Marek (2017) pointed out that horizontal and vertical cracks caused by temperature, pressure from stored materials, live loads, and other factors reduce the carrying capacity of silo walls, thereby reducing reliability. Lydia et al. (2019) proposed through numerical simulation that temperature loads are

the main cause of crack formation, and temperature transfer through the wall thickness is nonlinear. (Song, 2014; Guo, 2013; Yang and Ma, 2016; Ma et al., 2021; Ma and Yang, 2016) studied the temperature effects on steel silos and analyzed the temperature field of steel silos, concluding that the temperature field of the silo wall is uniformly distributed along the silo wall axis and varies trigonometrically across the cross-section. They also suggested that the temperature effect caused by solar radiation cannot be ignored in design. Zhang (2008) found that the largest impact among temperature loads is the internal and external temperature difference. The larger the temperature difference, the greater the displacement and stress. He also suggested increasing hoop reinforcement in the silo wall to ensure structural safety. Zheng et al., (2023) found that high temperature impacts on the overall performance of fully recycled aggregate concrete, necessitating an investigation of its mechanical property decay to understand damage mechanisms, with measures proposed to enhance high-temperature resistance and comprehensive summaries provided on thermodynamic parameters and computational models.

By employing advanced finite element analysis techniques using ABAQUS, the study provides a detailed understanding of stress distributions and deformation patterns under temperature loads, offering valuable insights for optimizing structural design under variable environmental conditions. The research bridges a gap in knowledge by highlighting the disparities in structural response under temperature rise and fall, emphasizing the need for targeted design strategies to mitigate stress concentrations, particularly in critical areas. The findings contribute to safer and more efficient construction practices, serving as a reference for engineers and researchers involved in designing resilient underground structures.

## 2. METHODOLOGY

In accordance with the Chinese “Standard for design of reinforced concrete silos” (GB 50077-2017) (2017), this paper presents the formula for calculating the horizontal lateral pressure induced by wall contraction due to temperature variations. Additionally, it stipulates a method for computing temperature-induced effects when the internal and external temperature difference is less than 100°C. For silos with diameters ranging from 12 to 30m, when accurate calculations of temperature effects are unobtainable and

practical experience is lacking, the temperature effect is calculated as 6% to 8% of the maximum hoop tension from the stored material load. For diameters exceeding 30m, the calculation of temperature stress follows Articles 4.3.1 to 4.3.10 of the standard. Among these, Article 4.3 specifies that the calculated results of temperature stress in reinforced concrete silos should be multiplied by a stiffness reduction coefficient. When the seasonal temperature differences between the interior and exterior surfaces of the silo or cylindrical wall are the same, the formula for calculating the temperature force  $p_c$  (kN/m) per unit area at the mid-plane of the wall is as follows:

$$p_c = \alpha_t \cdot \Delta T \cdot E \cdot h \quad (1)$$

where  $\alpha_t$  is the linear expansion coefficient of the silo wall or cylindrical wall;  $E$  is the elastic modulus of the silo wall or cylindrical wall;  $h$  is the thickness of the silo wall or cylindrical wall.

The formula for calculating the thermal gradient due to unbalanced temperature fields in the inner and outer walls of a silo is as follows:

$$T_D = \frac{T_s - T_a}{R_0} R_n \quad (2)$$

$$R_0 = \frac{1}{\alpha} + \frac{h_1}{\lambda_1} + \frac{h_2}{\lambda_2} + \frac{1}{\alpha_k} \quad (3)$$

where  $T_D$  is the temperature gradient resulting from heat conduction;  $R_0$  is the total thermal resistance;  $R_n$  is the thermal resistance of the  $n$ -th segment;  $\alpha$  and  $\alpha_k$  are the heat absorption and heat dissipation conduction coefficients;  $\lambda_1$  and  $\lambda_2$  are the thermal conduction coefficients of the stored material and the silo wall.

The formulas for calculating the maximum hoop stress  $\sigma_{\theta\max}$  and the maximum vertical stress  $\sigma_{z\max}$  per unit area on the inner and outer surfaces of a silo wall or cylindrical wall are as follows:

$$\sigma_{\theta\max} = \frac{\alpha_t \cdot \Delta T \cdot E}{2(1 - \mu_c)} \quad (4)$$

$$\sigma_{\theta\max} = \sigma_{z\max} \quad (5)$$

where  $\mu_c$  is poisson 's ratio of materials.

### 3. 3D FINITE ELEMENT ANALYSIS

#### 3.1 Model Construction

The calculation software employed is the internationally leading general-purpose finite element analysis software, ABAQUS.

The overall cylindrical coordinate system *ORTZ* conforms to the right-hand rule: it is stipulated that the vertical direction pointing upwards is taken as the positive direction of the *Z*-axis, with *R* and *T* representing the radial and tangential directions of the structure, respectively. The origin of the coordinate axes is located at the center of the circle where the vertical coordinate is 0. The concrete cylinder has a height of 60m, a baseplate thickness of 5m, an inner diameter of 29m, and a wall thickness of 0.5m, and is poured with C40 concrete.

To mitigate the impact of disturbances in the surrounding soil, the soil scope is defined as follows: a circle with a radius of 40m in both horizontal directions and vertically extending to an elevation of -120m. The displacements in the *X*, *Y*, and *Z* directions of the bottom soil are constrained, while the displacements in the *X* and *Y* directions of the lateral soil are constrained. The ground soil surface is a free surface and is not constrained. Both the foundation and the concrete structure are discretized into three-dimensional solid elements, and a finite element model is established according to the actual design dimensions. The calculation does not consider the displacement caused by the self-weight of the soil; instead, the initial stress conditions are applied as structural loads on the corresponding nodes and elements to balance the displacement resulting from the soil's self-weight and retain its initial stress (Bathe, 2006).

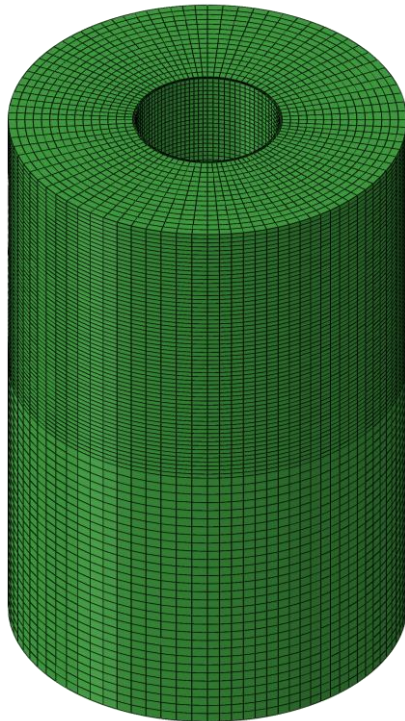


Fig. 1. Overall model

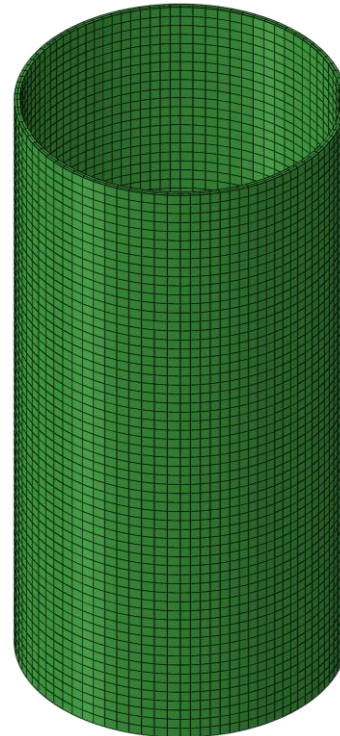


Fig. 2. Concrete cylinder model

Table 1 Material properties

| Material type | Density $\rho$ (kg/m <sup>3</sup> ) | Young's modulus $E$ (Pa) | Poisson's Ratio $\nu$ | Coefficient of linear expansion $\alpha_c$ (°C <sup>-1</sup> ) | Thermal conductivity $\lambda_c$ (J/(m·s·°C)) | Specific heat capacity $C_c$ (J/(kg·°C)) |
|---------------|-------------------------------------|--------------------------|-----------------------|--|---|--|
| Foundation    | 2500                                | $1.000 \times 10^{10}$   | 0.230                 | -  | -   | 750                                      |
| C40 concrete  | 2500                                | $3.250 \times 10^{10}$   | 0.167                 | $1.0 \times 10^{-5}$   | 2.94  | 960                                      |

The concrete structures are discretized into hexahedral eight-node three-dimensional solid elements, using a temperature-displacement coupling analysis step with element type C3D8RT, totaling 170950 elements and 180036 nodes. Fig. 1 illustrates the constructed overall model, and Fig. 2 depicts the concrete cylinder model. The parameters for the foundation and concrete materials are listed in Table 1.

### 3.2 Working condition and

The working conditions and load classifications are as follows:

- (1) Temperature increase: Self-weight + Temperature load (heating).
- (2) Temperature decrease: Self-weight + Temperature load (cooling).

The simulation is conducted using Steady-state coupled temp-displacement, with the self-weight referring to the weight of the concrete cylinder itself. For the temperature load, the initial temperature is set at 25°C. Below a depth of 10m from the ground surface, the soil temperature is essentially constant, assumed to be 25°C. When the temperature increases, a temperature boundary condition of 35°C is applied to the top of the cylinder; conversely, when the temperature decreases, a temperature boundary condition of 15°C is set at the top of the cylinder.

## 4. RESULTS AND DISCUSSION

### 4.1 Numerical Simulation Results

#### 4.1.1 Temperature increase

As shown in Fig. 3, the temperature field of the concrete cylinder during temperature increase is depicted. Fig. 4 presents the stress contour plot of the concrete cylinder. The influence of temperature rise load on the concrete cylinder is relatively small. Under the action of temperature rise load, the concrete cylinder is mainly subjected to compressive stress, and the stresses in all directions meet the concrete strength requirements. Fig. 5 illustrates the stress-elevation curve on the outer surface of the cylinder wall.

#### 4.1.2 Temperature decrease

As shown in Fig. 6, the temperature field of the concrete cylinder during temperature decrease is depicted. Fig. 7 presents the stress contour plot of the concrete cylinder. The temperature drop load has a significant impact on the concrete cylinder, particularly in the region between elevations of 0 and -3m, where the hoop tensile stress in the cylinder wall exceeds the standard axial tensile strength of the concrete, peaking at 2.75 MPa, which requires special attention. Fig. 8 illustrates the stress-elevation curve on the outer surface of the cylinder wall.

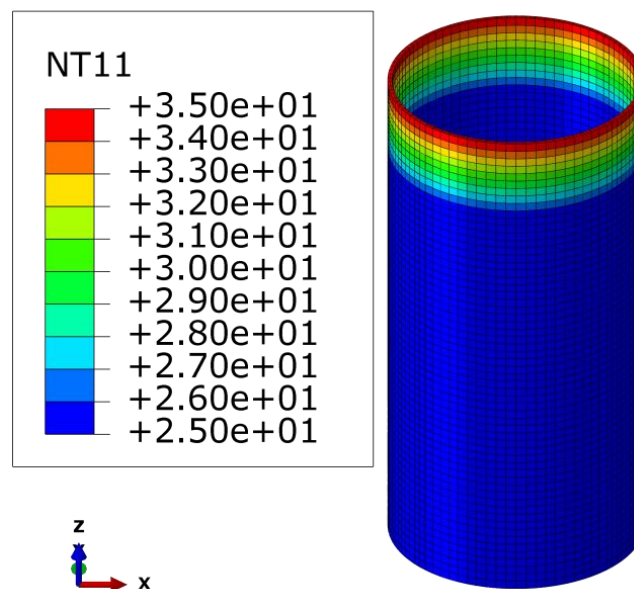


Fig. 3. Temperature field of concrete cylinder under temperature increase (unit: °C)

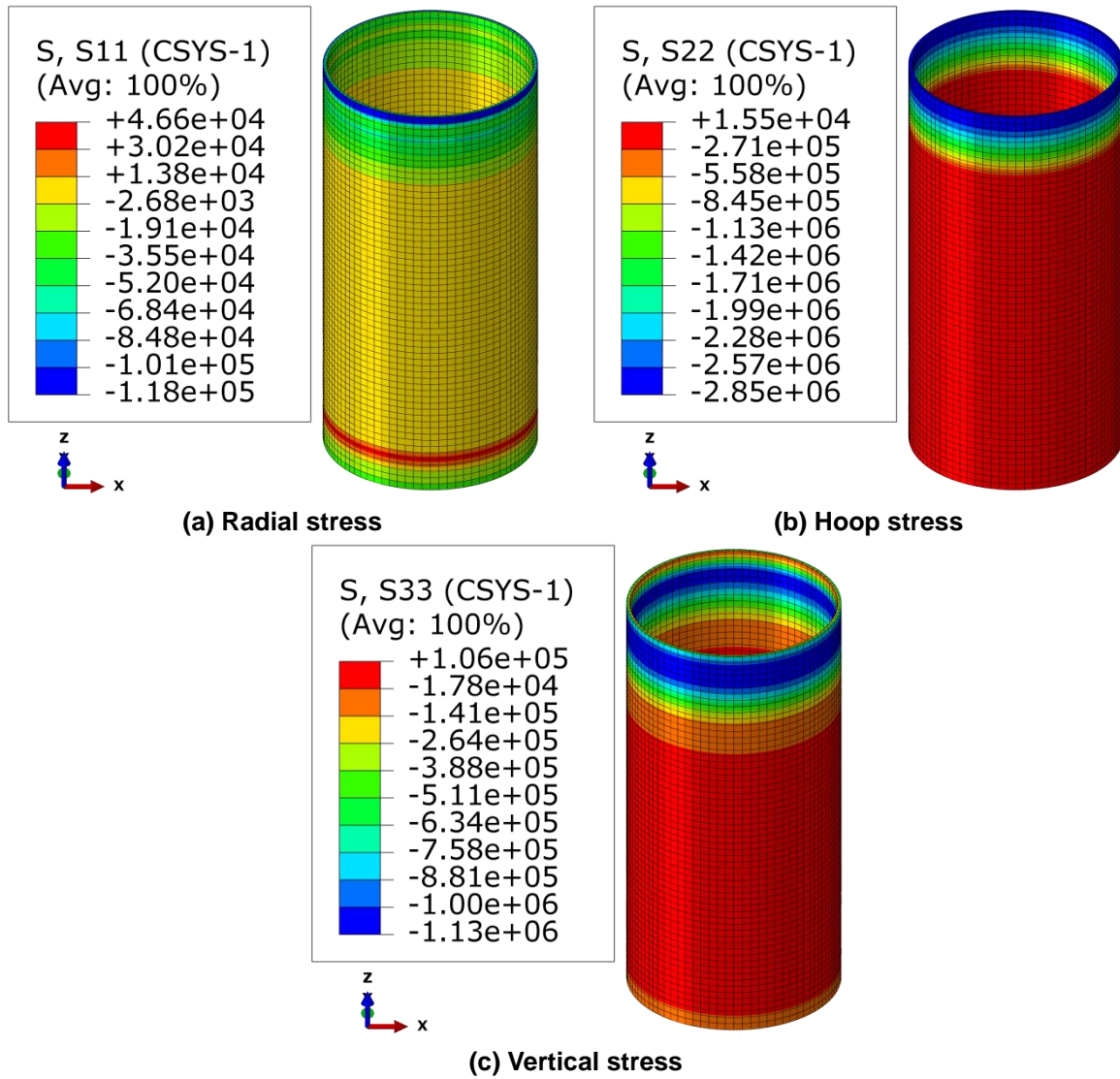


Fig. 4. (a,b & c) Stress of concrete cylinder under temperature increase (unit: Pa)

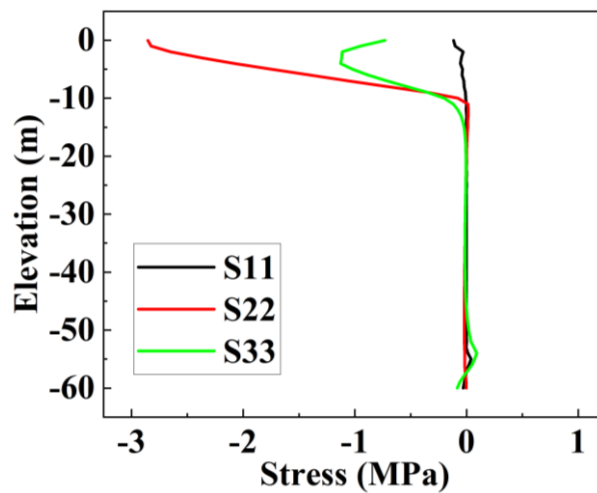


Fig. 5. Stress-elevation curve of concrete cylinder wall under temperature increase (unit: Pa)

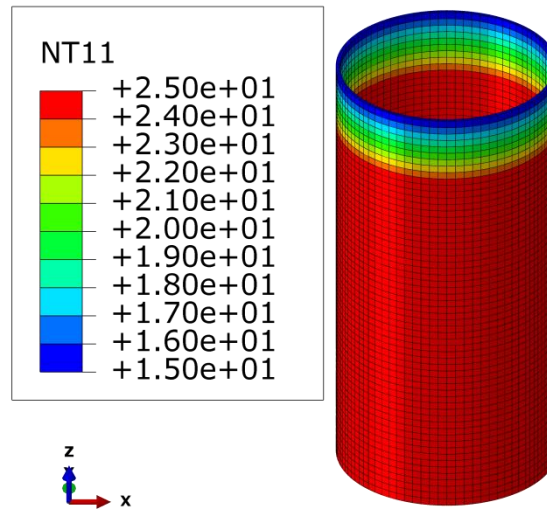


Fig. 6. Temperature field of concrete cylinder under temperature decrease (unit: °C)

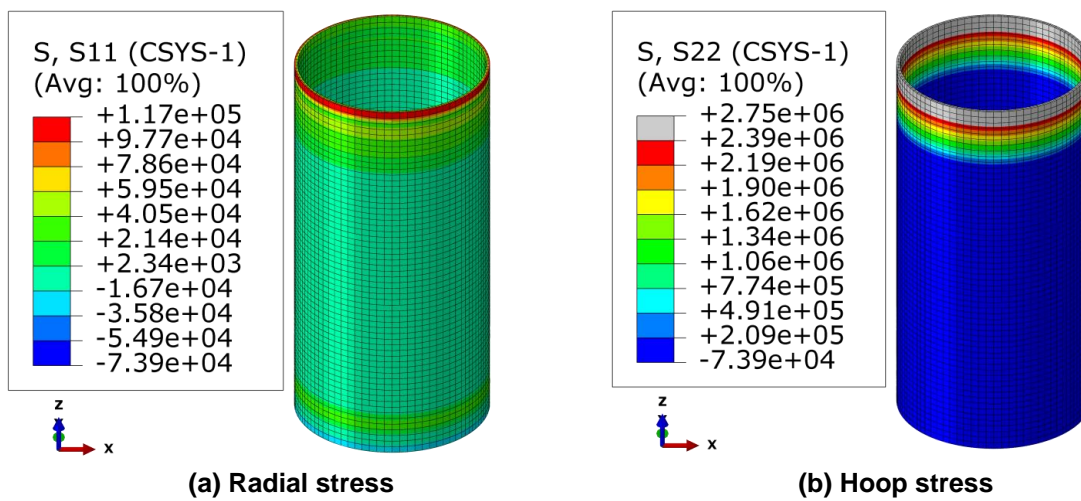


Fig. 7. (a & b) Stress of concrete cylinder under temperature decrease (unit: Pa)

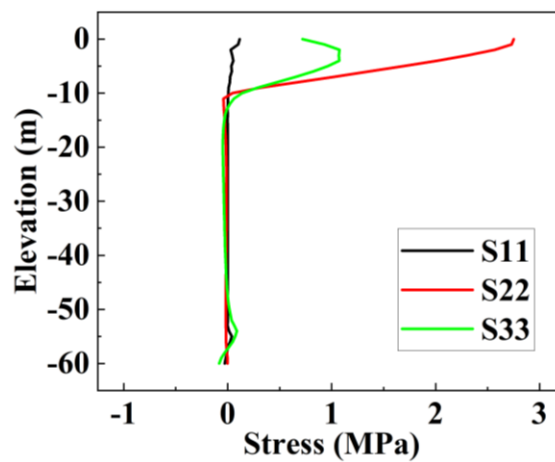


Fig. 8. Stress-elevation curve of concrete cylinder wall under temperature decrease (unit: Pa)

## 5. CONCLUSION

In this paper, a thorough investigation into the temperature stress distribution and deformation of a large-diameter underground concrete cylinder subjected to temperature loads is conducted using the finite element analysis (FEA) method and the advanced FEA software ABAQUS. During the research process, an accurate three-dimensional finite element model is constructed, considering the interaction between the concrete cylinder and the surrounding soil, and reasonable temperature boundary conditions are applied to simulate changes in temperature loads.

(1) The results show that during temperature increases, the concrete cylinder experiences compressive stress, with all stress values remaining within the material's strength limits. In contrast, the impact of temperature decrease conditions on the concrete cylinder is more significant, particularly in the region of the cylinder wall between elevations of 0 and -3m, where the hoop tensile stress exceeds the standard axial tensile strength of the concrete, peaking at 2.75 MPa. This finding highlights the need to pay special attention to the issue of hoop tensile stress concentration that may arise during temperature decrease in the design of large-diameter underground concrete cylinders and to adopt corresponding engineering measures to enhance the tensile capacity of this area, such as increasing the hoop reinforcement of the wall.

(2) Furthermore, by comparing the stress contour plots and stress-elevation curves under temperature increase and decrease conditions, it can be observed that temperature loads have a significant impact on the stress distribution and deformation of the concrete cylinder. Therefore, in the structural design and construction of large-diameter underground concrete cylinders, the effect of temperature loads must be fully considered to ensure the safety and stability of the structure.

In summary, the research in this paper not only provides in-depth insights and understanding into the mechanical characteristics of large-diameter underground concrete cylinders subjected to temperature loads but also offers valuable references and guidance for the design and construction of such structures. In future research, we can further explore more accurate temperature load simulation methods and more efficient finite element analysis tools to further

improve the scientificity and accuracy of the structural design and construction of large-diameter underground concrete cylinders.

## DISCLAIMER (ARTIFICIAL INTELLIGENCE)

Author(s) hereby declare that NO generative AI technologies such as Large Language Models (ChatGPT, COPILOT, etc) and text-to-image generators have been used during writing or editing of this manuscript.

## COMPETING INTERESTS

Author has declared that no competing interests exist.

## REFERENCES

- Bai, Y. J., Su, H., Bai, Y., et al. (2022). Mechanical properties and damage mechanisms of concrete under four temperature gradients combined with acoustic emission method. *Journal of Building Engineering*, 57, 104906.
- Bathe, K. J. (2006). *Finite element procedures*. Klaus-Jurgen Bathe.
- GB 50077-2017. (2017). *Standard for design of reinforced concrete silos*.
- Guo, H. W. (2013). The finite element analysis of temperature effects on large flat-bottom squat steel silos. (Master's thesis, Shandong University). Jinan.
- Guo, Y. L. (2018). Study on Temperature Effect of Construction Process of Large Diameter Reinforced Concrete Silo. (Doctoral dissertation, North China University of Water Resources and Electric Power). Zhengzhou.
- Khalifa, W. M. A., & El-Kashif, K. F. O. (2019). Computational Model for the Evaluation of Reinforced Concrete Silos Subjected to Thermal Load. *Engineering, Technology & Applied Science Research*, 9(4), 4411-4418.
- Kong, D. R., & Pu, W. M. (1998). Study on temperature effect of 40 m diameter cylindrical coal bunker. *Special Structures*, (2), 32-38+2.
- Lydia, M., Juraj, B., & Julius, S. (2019). Failure analysis of reinforced concrete walls of cylindrical silos under elevated temperatures. *Engineering Failure Analysis*, 109.
- Ma, Y., & Yang, Y. H. (2016). Temperature field of large flat-bottom silos under solar radiation. *Spatial Structures*, 22(4), 71-77.

- Ma, Y., Yang, H. X., Li, S. B., et al. (2021). Thermal Effects on the Coupled Thermo-Mechanical Buckling Behavior of Large Flat-Bottom Steel Silos. *Progress in Steel Building Structures*, 23(5), 37-44.
- Marek, M. (2017). Some Causes of Reinforced Concrete Silos Failure. *Procedia Engineering*, 172, 685-691.
- Morán, J. M., Juan, A., Ayuga, F., et al. (2005). Analysis of thermal load calculations in steel silos: A comparison of Eurocode 1, classical methods, and finite element methods. 48(4), 1483-1490.
- Morán, J. M., Juan, A., Robles, R., et al. (2006). Effects of environmental temperature changes on steel silos. *Biosystems Engineering*, 94(2), 229-238.
- Peng, X. F., & Fan, Y. (2020). Finite element analysis of large prestressed concrete coal storage silo. *Engineering Journal of Wuhan University*, 53(S1), 471-475.
- Song, J. (2014). Mechanical behavior analysis of large silos storage for high temperature stored materials. (Master's thesis, Zhejiang University). Hangzhou.
- Wang, D. B., Song, X. B., & Nie, H. Y. (2022). Cracking analysis of massive concrete with large-diameter pipes during construction. *Construction and Building Materials*, 338, 127636.
- Xia, G. Z., & Xia, D. T. (2006). Finite element analysis of giant reinforced concrete coal silos subject to temperature load. *Spatial Structures*, (1), 62-64+42.
- Yang, Y. H., & Ma, Y. (2016). A study on the temperature field of steel silos under solar radiation. *J. Xi'an Univ. of Arch. & Tech. (Natural Science Edition)*, 48(1), 52-57.
- Zhang, S. K. (2008). Temperature load and storage material load finite element analysis of large-diameter reinforced concrete silo. (Master's thesis, Wuhan University of Technology). Wuhan.
- Zhang, Y. (2010). The Finite Element Analysis of Temperature Effects on Large-diameter Ground-supported Flat-bottomed Cylindrical Steel Silo. (Doctoral dissertation, Xi'an University of Architecture and Technology). Xi'an.
- Zhangabay, N., Suleimenov, U., Utebayeva, A., et al. (2023). Experimental research of the stress-strain state of prestressed cylindrical shells taking into account temperature effects. *Case Studies in Construction Materials*, 18, e01776.
- Zhao, L., Yang, Z. Y., & Wang, L. J. (2018). Investigation on the non-uniform temperature distribution of large-diameter concrete silos under solar radiation. *Mathematical Problems in Engineering*, (3), 1-16.
- Zheng, Y., Xi, X., Zhang, Y., et al. (2023). Review of mechanical properties and strengthening mechanism of fully recycled aggregate concrete under high temperature. *Construction and Building Materials*, 394, 132221.

**Disclaimer/Publisher's Note:** The statements, opinions and data contained in all publications are solely those of the individual author(s) and contributor(s) and not of the publisher and/or the editor(s). This publisher and/or the editor(s) disclaim responsibility for any injury to people or property resulting from any ideas, methods, instructions or products referred to in the content.

© Copyright (2025): Author(s). The licensee is the journal publisher. This is an Open Access article distributed under the terms of the Creative Commons Attribution License (<http://creativecommons.org/licenses/by/4.0>), which permits unrestricted use, distribution, and reproduction in any medium, provided the original work is properly cited.

Peer-review history:

The peer review history for this paper can be accessed here:

<https://www.sdiarticle5.com/review-history/129614>